



Aniruddha Hemantkumar Wadekar
464438

Assignment-1 Introduction to Fluid Mechanics and Heat
Transfer

School of Aerospace, Transport and Manufacturing
Computational Fluid Dynamics

MSc
Academic Year: 2024–2025

Supervisor: Dr. László Könözy
November 2024

© Cranfield University 2024. All rights reserved. No part of this publication may be reproduced without the written permission of the copyright owner.

Academic Integrity Declaration

I declare that:

- the thesis submitted has been written by me alone.
- the thesis submitted has not been previously submitted to this university or any other.
- that all content, including primary and/or secondary data, is true to the best of my knowledge.
- that all quotations and references have been duly acknowledged according to the requirements of academic research.

I understand that to knowingly submit work in violation of the above statement will be considered by examiners as academic misconduct.

Abstract

This report investigates the development of fully developed laminar flow in a two-dimensional narrow rectangular channel with non-slip condition and a constant Reynolds number. The study begins with the derivation of the governing equations, specifically the incompressible form of the Navier-Stokes equations in three dimensions, which are subsequently simplified to suit the conditions of the current investigation. The resulting analytical solution is implemented in MATLAB to obtain the velocity profile for the specified geometry. Numerical simulations are performed in ANSYS Fluent using a two-dimensional rectangular grid with three different grid resolutions. The results from these simulations are quantitatively compared with the analytical solution to determine the change in accuracy of the solution with change in grid resolution. Furthermore, the effect of non-isothermal boundary conditions on the velocity profile and the temperature distribution is analysed through both numerical and analytical methods. Finally, the report presents a detailed comparison of absolute and relative errors between the numerical and analytical solutions, providing insights into the accuracy and reliability of the results. Keywords:

Hagen-Poiseuille Flow; 2D Laminar flow; Navier-Stokes equations; Analytical solution v/s Numerical solution

Table of Contents

Academic Integrity Declaration	i
Abstract	ii
Table of Contents	iii
List of Figures	iv
List of Tables	v
Nomenclature	vi
1 Introduction	1
1.1 Assumptions	2
1.2 Given Data	2
1.3 Geometry	3
2 Governing Equations and its Solution	4
2.1 Continuity Equation	4
2.2 Navier-Stokes Equation for Icompressible flow	4
2.3 X, Y and Z - Momentum Equation	4
2.4 Velocity Equation	5
2.5 Pressure Difference Equation	6
3 Results and Discussion	7
3.1 Analytical Solution	7
3.2 Numerical Simulations	8
3.2.1 Model Setup	8
3.2.2 Results and Discussions	9
3.2.2.1 Outflow Condition - 2 nd Order	9
3.2.2.2 Pressure Outlet Condition - 2 nd Order	10
3.2.2.3 1 st Order v/s 2 nd Order Comparison	10
3.2.2.4 Non Isothermal Solution	11
3.2.2.5 Error	12
4 Conclusion	13
References	14

List of Figures

1.1	Representation of the Geometry considered	3
3.1	Analytical Velocity Profile	7
3.2	Model Setup in ANSYS Fluent	8
3.3	Coarse grid - Residual Plot	9
3.4	Mdeium grid - Residual Plot	9
3.5	Fine grid Residual Plot	9
3.6	Outflow 2 nd Order - Comparison	10
3.7	Pressure Outlet 2 nd Order - Comparison	10
3.8	Outflow Condition 1st Order v/s 2nd Order	11
3.9	Pressure Outlet Condition 1st Order v/s 2nd Order	11
3.10	Temp Distribution in domain	11
3.11	Temp Distribution at outlet	11
3.12	Absolute Error Bar Chart	12
3.13	Relative Error Bar Chart	12

List of Tables

3.1	Grid Resolutions	8
3.2	Number of Numerical Simulations per Grid	9

Nomenclature

1. CFD – Computational Fluid Dynamics
2. N-S – Navier-Stokes Equation
3. 2D – 2 Dimensional
4. ρ – Fluid Density (kg/m^3)
5. L – Channel Length (m)
6. H – Channel Height (m)
7. u, v, w – Velocity Components in X, Y and Z directions Respectively m/s
8. $\nabla = \vec{e}_x \frac{\partial}{\partial x} + \vec{e}_y \frac{\partial}{\partial y} + \vec{e}_z \frac{\partial}{\partial z}$
9. t – Time
10. g – Gravity (m/s)
11. P – Pressure (Pa)
12. μ – Dynamic Viscosity ($Pa.s$)
13. ν – Kinematic Viscosity m^2/s
14. $u(y)$ – Velocity function in Y direction (m/s)
15. u_{max} – Maximum velocity (m/s)
16. u_{avg} – Average velocity (m/s)
17. Re – Reynolds number
18. Q – Volume Flow rate (m^3/s)
19. W_{ch} – Width of the Channel m
20. ΔP – Pressure Drop (Pa)
21. l_e – Hydrodynamic Development Length / entrance length (m)
22. α – Thermal Diffusivity m^2/s

- 23. C_p – Specific Heat Constant J/kgK
- 24. T_L – Temperature at lower wall K
- 25. T_U – Temperature at upper wall K
- 26. A_{error} – Absolute Error
- 27. S_{value} – Maximum Simulated Value
- 28. A_{value} – Maximum Analytical value
- 29. R_{error} – Relative Error
- 30. u_{amx} – Maximum velocity obtained from Analytical Solution(for Graph only)
- 31. u_{smx} –Maximum velocity obtained from Numerical Solution(for Graph only)

Chapter 1

Introduction

Fluid Mechanics is one of the foundation pillars in engineering. Any material that flows is classified as a fluid. Over the decades, the study of fluid behavior has evolved significantly, however, certain classical problems have remained central to both theoretical and applied studies. Among these is the investigation of laminar flow between two stationary parallel plates also referred to as Hagen-Poiseuille flow (5). With minor modifications, this can be scaled to solve problems within circular pipes as well. Due to its simplicity, and versatility, the Hagen-Poiseuille flow can be used in numerous applications where precise control over the flow conditions is required.

This study focuses on deriving the analytical solution for steady-state, incompressible, viscous laminar flow in a two-dimensional (2D) channel. The problem assumes no-slip boundary conditions, where the fluid velocity at the solid boundaries equals that of the walls. This assumption is fundamental in viscous flows, as it captures the interactions between the fluid and the surface at the molecular level. The resulting velocity profile is parabolic, representing the balance between viscous forces and pressure-driven flow, which are dominant in low Reynolds number regimes. Additionally, the flow is assumed to be non-vortical in the fully developed region, where the velocity gradient in the axial direction becomes negligible. The Reynolds number plays a big part throughout the process. Almost all analytical data are in some way dependent on the Reynolds number. As common knowledge, for laminar flow, the Reynolds number should be below 2000. In the current problem statement, the Reynolds number considered is 350.

The analytical solution is derived from the governing equations of fluid dynamics—the momentum equations, more commonly referred to as the Navier-Stokes (N-S) equations. The derived equation defines the velocity distribution in the channel under the assumption of steady-state, two-dimensional flow. Further numerical simulations are carried out using commercial CFD software package – ANSYS Fluent for a range of grid sizes. The results observed are then compared to obtain a quantitative metric for accuracy of the numerical solutions to the analytical one. This is done by comparing the absolute and relative errors for the obtained solutions.

During the process, it was observed that the initial dimensions provided for the geometry needed adjustment. This was with respect to the Hydrodynamic Development length commonly referred to as ‘entrance length’ (3)(1). The initial length of the channel given in the problem statement is not sufficient to observe a fully developed flow. Hence the length of the channel was altered so as to facilitate the observation of the fully developed

flow.

Non-Isothermal boundary conditions are taken into effect to observe the temperature distribution. This can be useful in determining the energy transfer that happens between the fluid molecules as it flows within a region of boundaries maintained at different temperatures. The Temperature distribution was then plotted using MATLAB to obtain a visual representation of the phenomenon.

1.1 Assumptions

Before starting with the exercise, some assumptions about the fluid flow have been made. They are listed as follows

1. Flow is 2D Steady State, and Incompressible hence

$$\frac{\partial \vec{u}}{\partial t} = 0$$

$$\nabla \cdot \vec{u} = \frac{\partial u}{\partial x} + \frac{\partial v}{\partial y} = 0$$

2. Velocity Components in Y and Z directions are neglected $v = w = 0$
3. Velocity of of walls is zero and No Slip boundary condition
4. Pressure Drop remains Constant throughout the channel
5. Effect of Gravity is Neglected $g = 0$
6. Change in Flux is zero

1.2 Given Data

1. Density of the Fluid $\rho = 1000 \text{ kg/m}^3$
2. Dynamic Viscosity $\mu = 0.00102 \text{ Pa.s}$
3. Reynolds number $Re = 350$
4. Kinematic Viscosity $\frac{\mu}{\rho} = (2.9142)10^{-6} \text{ m}^2/\text{s}$
5. Channel Height $H = 0.45 \text{ m}$
6. Channel Length $L = 0.25 \text{ m}$
7. Thermal Diffusivity $\alpha = (0.143)10^{-6} \text{ m}^2/\text{s}$
8. Specific Heat Constant $C_p = 4185 \text{ J/kgK}$
9. Temperature at lower wall $T_L = 50 \text{ K}$
10. Temperature at upper wall $T_U = 350 \text{ K}$

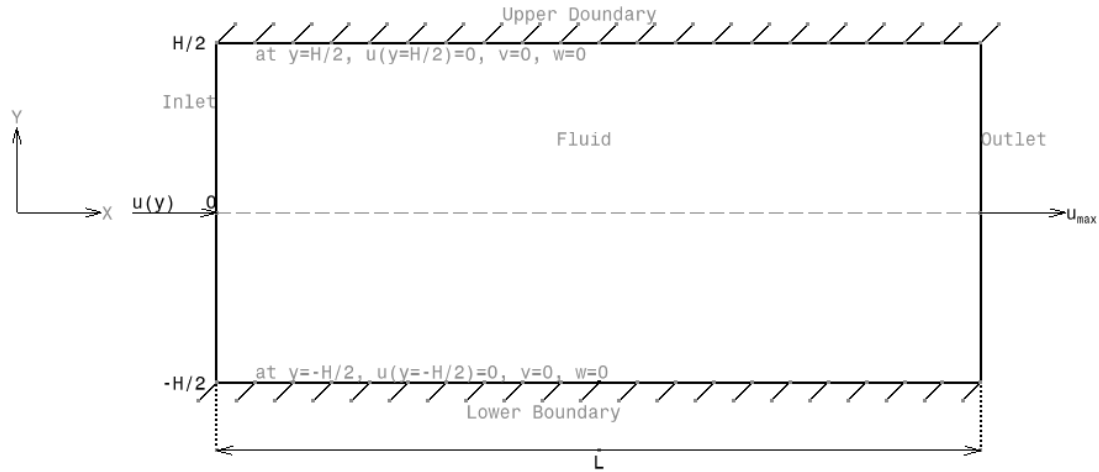


Figure 1.1: Representation of the Geometry considered

1.3 Geometry

The figure 1.1 shows the arrangement of the geometry. The two flat parallel plates are fixed on either sides of the X-Axis at distance of $H/2m$ each. The fluid will enter from the inlet and flow towards the outlet. As the plates are fixed and no slip condition is assumed, the velocity component at the wall boundaries is equal to zero. Looking at the geometry, theoretically, the velocity profile should be a parabolic curve.

Chapter 2

Governing Equations and its Solution

2.1 Continuity Equation

$$\frac{du}{dx} = 0 \quad (2.1)$$

2.2 Navier-Stokes Equation for Icompressible flow

$$\frac{\partial u}{\partial t} + (\vec{u} \nabla) \vec{u} = g - \left[\frac{1}{\rho} \nabla P \right] + \nu \nabla^2 \vec{u} \quad (2.2)$$

2.3 X, Y and Z - Momentum Equation

The Eq.2.2 can be further broken down into X, Y and Z directions.
Momentum Equation in X-Direction is-

$$u \frac{\partial u}{\partial x} + v \frac{\partial u}{\partial y} + w \frac{\partial u}{\partial z} = -\frac{1}{\rho} \frac{\partial P}{\partial x} + \nu \left(\frac{\partial^2 u}{\partial x^2} + \frac{\partial^2 u}{\partial y^2} + \frac{\partial^2 u}{\partial z^2} \right) \quad (2.3)$$

Momentum Equation in Y-Direction is-

$$u \frac{\partial v}{\partial x} + v \frac{\partial v}{\partial y} + w \frac{\partial v}{\partial z} = -\frac{1}{\rho} \frac{\partial P}{\partial y} + \nu \left(\frac{\partial^2 v}{\partial x^2} + \frac{\partial^2 v}{\partial y^2} + \frac{\partial^2 v}{\partial z^2} \right) \quad (2.4)$$

Momentum Equation in Z-Direction is-

$$u \frac{\partial w}{\partial x} + v \frac{\partial w}{\partial y} + w \frac{\partial w}{\partial z} = -\frac{1}{\rho} \frac{\partial P}{\partial z} + \nu \left(\frac{\partial^2 w}{\partial x^2} + \frac{\partial^2 w}{\partial y^2} + \frac{\partial^2 w}{\partial z^2} \right) \quad (2.5)$$

Now as per given conditions, velocities along the Y and Z directions are zero, (refer equation in given data). Therefore, the equations in Y (eq. 2.4) and Z (eq. 2.5) direction can be neglected. Thus the X Momentum equation eq.2.3 can be further simplified as

$$0 = -\frac{1}{\rho} \frac{\partial P}{\partial x} + \nu \frac{\partial^2 u}{\partial y^2}$$

The pressure gradient is assumed constant along the flow direction.

$$-\frac{1}{\rho} \frac{\partial P}{\partial x} = \frac{\Delta P}{\rho L}$$

Therefore, the X momentum Equation now becomes

$$0 = \frac{\Delta P}{\rho L} + \nu \frac{d^2 u}{dy^2}$$

$$\nu \frac{d^2 u}{dy^2} = -\frac{\Delta P}{\rho L}$$

or by definition of kinematic viscosity 1.2

$$\frac{d^2 u}{dy^2} = -\frac{\Delta P}{\mu L} \quad (2.6)$$

2.4 Velocity Equation

To obtain the velocity equation $u(y)$, eq2.6 must be integrated twice with respect to 'y'

$$\begin{aligned} u(y) &= \iint -\frac{\Delta P}{\mu L} dy dy \\ u(y) &= -\frac{\Delta P}{\mu L} \left[\int (y + c_1) dy \right] \\ u(y) &= -\frac{\Delta P}{\mu L} \left[\frac{y^2}{2} + yc_1 + c_2 \right] \end{aligned} \quad (2.7)$$

Now from boundary values

at the lower wall boundary, $y = -\frac{H}{2}$ and $u(y) = 0$

Substituting this in eq.2.7

$$0 = -\frac{\Delta P}{\mu L} \left[\frac{H^2}{8} - \frac{H}{2} c_1 + c_2 \right] \quad (2.8)$$

at the upper wall boundary, $y = \frac{H}{2}$ and $u(y) = 0$

Substituting this in eq.2.7

$$0 = -\frac{\Delta P}{\mu L} \left[\frac{H^2}{8} + \frac{H}{2} c_1 + c_2 \right] \quad (2.9)$$

Solving eq.2.8 and eq.2.9 simultaneously we get values of c_1 and c_2 as

$$c_1 = 0 \quad (2.10)$$

$$c_2 = \frac{-H^2}{8} \quad (2.11)$$

Substituting eq.2.10 and eq.2.11 in eq.2.7 , the final velocity function becomes

$$u(y) = -\frac{\Delta P}{\mu L} \left[\frac{y^2}{2} - \frac{H^2}{8} \right] \quad (2.12)$$

For the given conditions, eq.2.12 gives the fully developed Laminar Velocity profile

2.5 Pressure Difference Equation

The Volume flow rate is given as

$$Q = W_{ch} \int_{-\frac{H}{2}}^{\frac{H}{2}} u(y) dy$$

From eq.2.12

$$\begin{aligned} Q &= W_{ch} \int_{-\frac{H}{2}}^{\frac{H}{2}} -\frac{\Delta P}{\mu L} \left[\frac{y^2}{2} - \frac{H^2}{8} \right] dy \\ Q &= W_{ch} \left(-\frac{\Delta P}{\mu L 2} \right) \left[\left[\frac{y^3}{3} \right]_{-\frac{H}{2}}^{\frac{H}{2}} - \left[\frac{yH^2}{4} \right]_{-\frac{H}{2}}^{\frac{H}{2}} \right] \\ Q &= W_{ch} \left(-\frac{\Delta P}{\mu L 2} \right) \left[\frac{H^3}{12} - \frac{H^3}{4} \right] \\ Q &= \left(\frac{W_{ch} H^3 \Delta P}{12 \mu L} \right) \end{aligned}$$

Rearranging the equation, we get

$$\Delta P = \frac{12 Q L \mu}{W_{ch} H^3}$$

Also, $Q = u_{avg} W_{ch} H$, hence, ΔP can be written as

$$\Delta P = \frac{12 u_{avg} L}{H^2} \quad (2.13)$$

This is the equation for computing the pressure drop for the said channel

Chapter 3

Results and Discussion

3.1 Analytical Solution

Now the average Velocity of the flow is given by

$$u_{avg} = \frac{vRe}{2H} = 0.000396667m/s \quad (3.1)$$

It is important to note that the for the given geometry the dimensions of the channel are very small. In such a case, the fully developed laminar flow is not observed. Hence, the original length of the channel is replaced with the hydrodynamic length also commonly know as entrance length For Laminar flow, the Hydro Dynamic Length is expressed as a function of the channel height and the Reynolds number

$$l_e = 0.06HRe \quad (3.2)$$

The effective length of the channel, accounting for entrance effects,

$$Length = L = l_e = 9.45m \quad (3.3)$$

Using equation 2.12 and given data, a graph of the velocity profile was plot using MATLAB program. As expected the velocity profile is parabolic in nature with the Maximum velocity at the center of the channel(along the symmetry line) and minimum at the

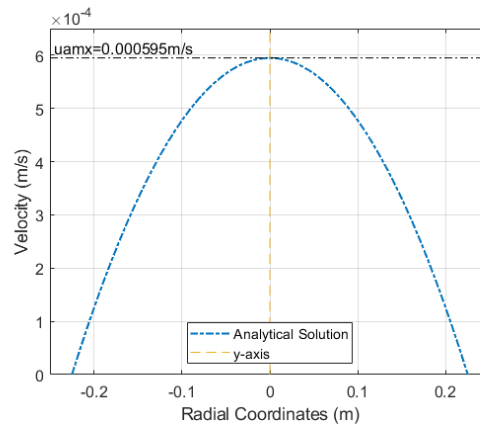


Figure 3.1: Analytical Velocity Profile

walls. Figure 3.1 shows the same profile. The radial coordinates(m) are taken along the X axis whereas the velocity(m/s) is plotted on the Y axis. The maximum observed velocity from the analytical solution is

$$u_{max} = 0.000595m/s \quad (3.4)$$

3.2 Numerical Simulations

3.2.1 Model Setup

To obtain the numerical solutions for to given problem, a commercial CFD software package ANSYS Fluent was used. The 2D geometry was prepared with the height(eq.??) and length (eq. 3.3).

This geometry was meshed in 3 different resolutions - coarse, medium and fine

Table 3.1: Grid Resolutions

grid Resolution	Number of Elements
Coarse grid	13875
Medium grid	52500
Fine grid	118125

These mesh files were loaded in ANSYS Fluent. After selecting the material properties as per given data 1.2 , the Viscous (Laminar) model was selected for the analysis. The boundary conditions were setup as per the given data. The inlet velocity of the fluid was obtained from eq.3.1 . Further, the residual convergence criterion was set to 10^{-6} . After setting up the models they were solved with close attention to the residual convergence. A small comparison was done between the residuals of the coarse, medium and fine mesh

Comparing the plots in Fig 3.3, 3.4, 3.5 it was observed that the convergence in all three

Ansyes
2024 R2



Figure 3.2: Model Setup in ANSYS Fluent

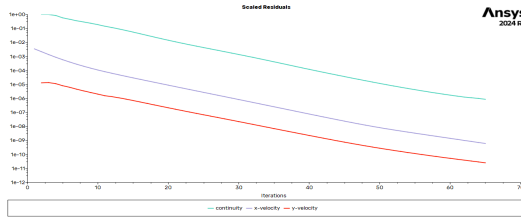


Figure 3.3: Coarse grid - Residual Plot

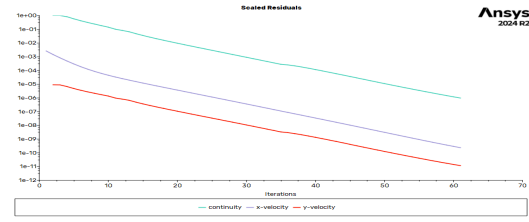


Figure 3.4: Medium grid - Residual Plot

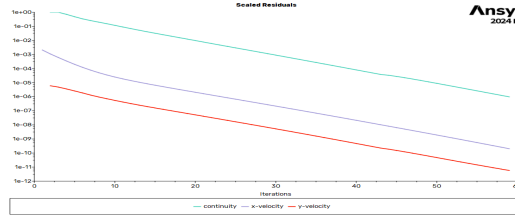


Figure 3.5: Fine grid Residual Plot

cases is very much the same. All three instances required almost the same number of iterations to achieve convergence.

3.2.2 Results and Discussions

The number of simulations run were as described below.

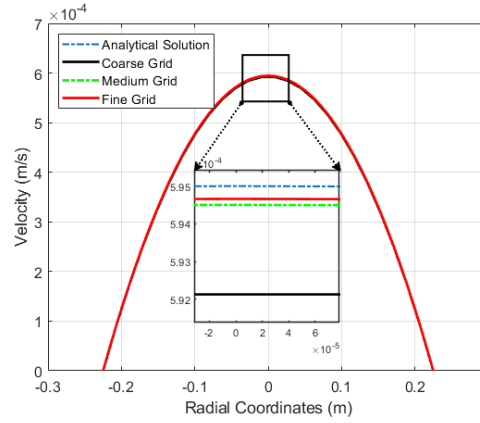
Table 3.2: Number of Numerical Simulations per Grid

Grid Type	Number of Simulations	Outflow Condition	Pressure-Outlet Condition	Non Isothermal Condition
Coarse Grid	4	1st and 2nd Order	1st and 2nd Order	-
Medium Grid	2	2nd Order	2nd Order	-
Fine Grid	3	2nd Order	2nd Order	1

3.2.2.1 Outflow Condition - 2nd Order

The results for the 3 grids were obtained and plotted along with the analytical solution (fig 3.6). As observed, the solution with the fine grid ($u_{fine} = 0.000594661m/s$) is closest to the ideal value ($u_{max} = 0.000595m/s$) followed by the medium ($u_{medium} = 0.000594503m/s$) and the coarse grid ($u_{coarse} = 0.000592132m/s$) respectively.

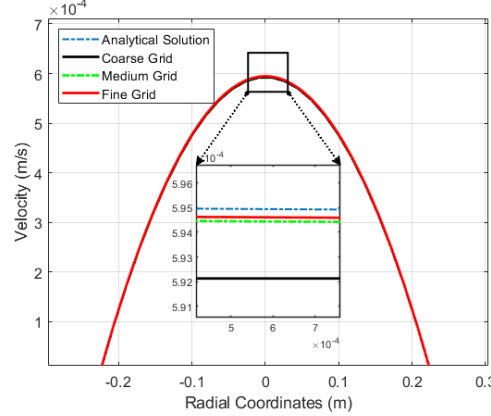
In terms of accuracy, the coarse solution is the most inaccurate out of the 3. The medium and the fine solutions are relatively better (3.2.2.5). The relative difference solution between the medium and the fine grid is very small (0.000000158). This can be considered as a criterion for deciding the grid size.

Figure 3.6: Outflow 2nd Order - Comparison

3.2.2.2 Pressure Outlet Condition - 2nd Order

The general trend of the results is similar to the observations mentioned in section 3.2.2.1. Also the velocity magnitude for all three grid sizes is comparable with the ones from the outflow condition. The relative difference between the observed values between the outflow and the pressure condition ($u_{outflow} - u_{pressure}$) is as small as 1×10^{-8} . The maximum values of the velocity are -

($u_{fine} = 0.00059466m/s$) , ($u_{medium} = 0.000594502m/s$) , ($u_{coarse} = 0.00059213m/s$)

Figure 3.7: Pressure Outlet 2nd Order - Comparison

3.2.2.3 1st Order v/s 2nd Order Comparison

For the coarse grid, 4 simulations were performed (refer table 3.2). The results are grouped under the Outflow and the Pressure Outlet condition. Refer Figures 3.8 and 3.9 the parabolic curves in both the graphs are similar in nature. The curves for 1st and 2nd order are almost coincident and the difference between them is of the order 1×10^{-8} . For the given problem, this is relatively very small.

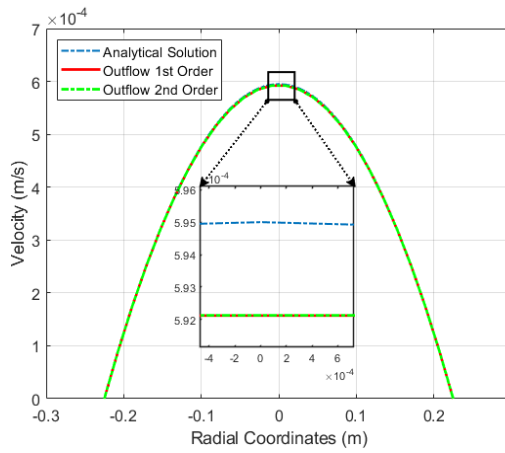


Figure 3.8: Outflow Condition 1st Order v/s 2nd Order

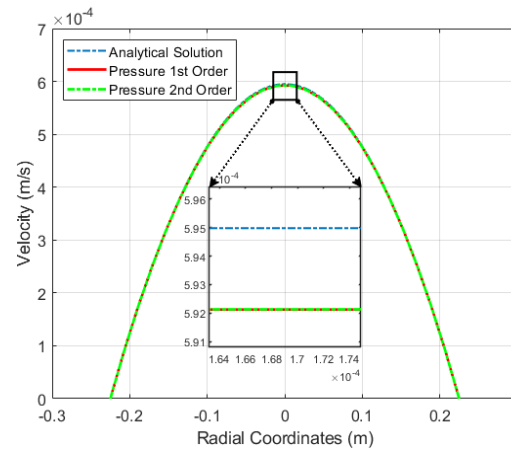


Figure 3.9: Pressure Outlet Condition 1st Order v/s 2nd Order

3.2.2.4 Non Isothermal Solution

A non isothermal solution was performed on the fine grid. Apart from the Viscous (Laminar) model, the Energy model was also selected. Note that this did not affect the velocity profile for the solution. The temperature boundary conditions were applied as per given data (refer section 1.2).

It was observed that throughout the channel, the temperature near the lower boundary

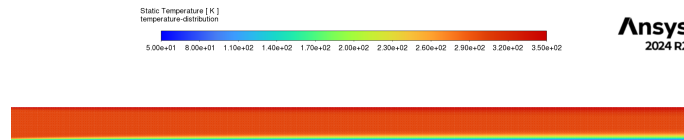


Figure 3.10: Temp Distribution in domain

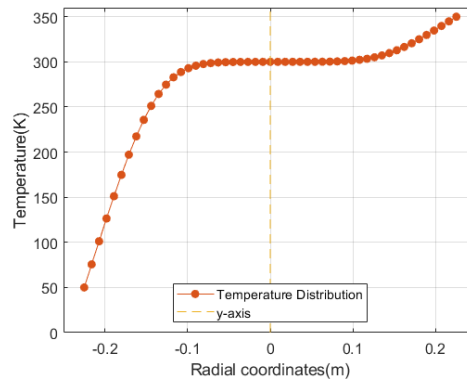


Figure 3.11: Temp Distribution at outlet

remains at a considerably lower level. As observed on the graph 3.11, the temperature rises steeply till it reached the central region (symmetry line.) It remains stable around 300K and later rises to 350K towards the upper wall boundary.

3.2.2.5 Error

Numerical Simulations are never exact simulations. At best they can be considered as approximate. Thus to quantify them, we need to check for errors. For the scope of this task, Absolute and Relative Error (%) were evaluated over the means of both the numerical result and the analytical solution. Absolute Error is obtained by the following formula

$$A_{error} = |u_{Amean} - u_{Nmean}| \quad (3.5)$$

where u_{Amean} is the mean velocity from the analytical results and u_{Nmean} is the mean velocity from the numerical results.

$$R_{error} = 100 * \left| \frac{A_{error}}{u_{Amean}} \right| \quad (3.6)$$

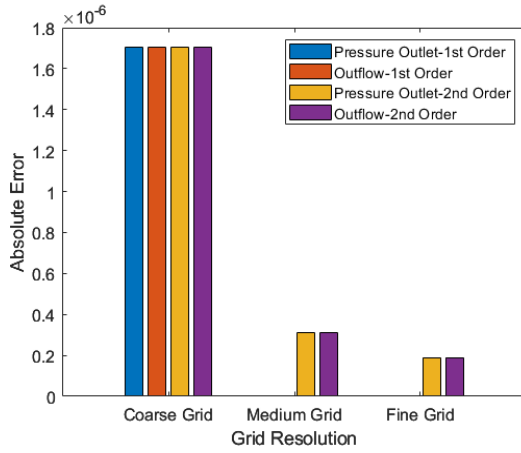


Figure 3.12: Absolute Error Bar Chart

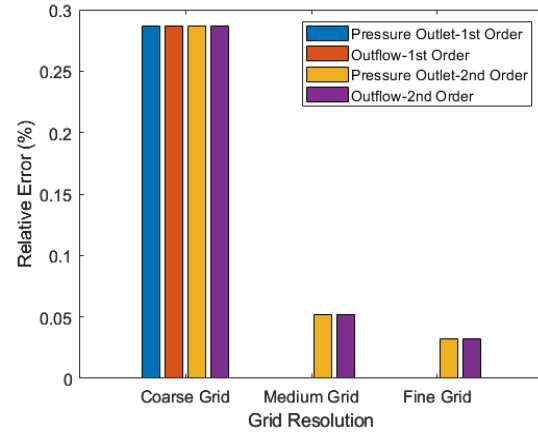


Figure 3.13: Relative Error Bar Chart

The graphs depict an easy trend. from the Absolute Error chart(3.12) it is clear that the coarse grid is the farthest away from the analytical solution by a value of $1.705 * 10^{-6}$. The fine grid has the least error of magnitude $1.897 * 10^{-7}$. The absolute error for the medium grid is slightly higher than the fine grid at $3.104 * 10^{-7}$

As the Relative error(fig3.13 depends on the absolute error, similar trends were noted as absolute error. Quantitatively, for fine grid, the relative error is 0.03188 % , for medium gird, it is 0.5217% and lastly the coarse grid 0.2865%.

It was also observed that the errors are independent about the 1st order and 2nd order or the type of outlet boundary condition. This comes down to the fact that the values of the velocities obtained from these simulations were almost identical to each other for the specific grid type(observed difference was of the order 10^{-8}).

Chapter 4

Conclusion

This report discussed the development of the Hagen-Poiseuille flow for viscous fluid in a narrow 2D rectangular channel. The governing equations were derived and the Analytical and Numerical simulations were carried out to obtain velocity profile of the fluid for 3 different mesh sizes. Additionally the obtained results were compared to obtain absolute and relative errors. The observations convey that the fine grid is the closest to the analytical solution followed closely by the medium grid and then the coarse grid. In case of residual convergence criterion, all 3 domains fared pretty much the same. Also, the change in the outlet boundary condition or the order of the equations had very minor effect on the results in this case. Additionally, a non isothermal simulation was studied to observe the temperature distribution within the fluid.

References

1. Mohanty, A. K., & Asthana, S. B. L. (1979). Laminar flow in the entrance region of a smooth pipe. *Journal of Fluid Mechanics*, 90(3), 433–447. <https://doi.org/10.1017/s0022112079002330>
2. Han, L. S. (1960). Hydrodynamic Entrance Lengths for Incompressible Laminar Flow in Rectangular Ducts. *Journal of Applied Mechanics*, 27(3), 403–409. <https://doi.org/10.1115/1.3644015>
3. Munson, B. R., Young, D. F., & Okiishi, T. H. (2007). *Fundamentals of Fluid Mechanics*. John Wiley & Sons.
4. Anderson, J. D. (2007). *Computational Fluid Dynamics: The Basics with Applications*. McGraw-Hill.
5. White, F. M. (2016). *Fluid Mechanics* (8th ed.). Mcgraw-Hill Education.